QUANTITATIVE X-RAY STRUCTURE DETERMINATION OF SUPERLATTICES AND INTERFACES

IVAN K. SCHULLER*, ERIC E. FULLERTON*, H. VANDERSTRAETEN**, AND Y. BRUYNSERAEDE**

*Physics Department 0319, University of California - San Diego, La Jolla, California 92093, USA

**Laboratorium voor Vaste Stof-Fysika en Magnetisme, Katholieke Universiteit Leuven, B-3001 Leuven, Belgium.

ABSTRACT

We present a general procedure for quantitative structural refinement of superlattice structures. To analyze a wide range of superlattices, we have derived a general kinematical diffraction formula that includes random, continuous and discrete fluctuations from the average structure. By implementing a non-linear fitting algorithm to fit the entire x-ray diffraction profile, refined parameters that describe the average superlattice structure, and deviations from this average are obtained. The structural refinement procedure is applied to a crystalline/crystalline Mo/Ni superlattices and crystalline/amorphous Pb/Ge superlattices. Roughness introduced artificially during growth in Mo/Ni superlattices is shown to be accurately reproduced by the refinement.

INTRODUCTION

The study of the structure of superlattice has received increased interest in recent years. Much of this interest is the result of the wide range of new physical phenomena observed in these systems. The presence of the additional periodicity of the layered material often leads to unique magnetic, transport, mechanical, and superconducting properties[1]. The understanding of the physical properties is limited by the characterization of the samples. Many of the physical properties depend sensitively on structural properties such as interdiffusion, crystallinity, strain, and roughness making structural characterization a prerequisite to understanding the physical properties.

X-ray diffraction is a technique that is well suited for studying the structure of superlattices. It is non-destructive and can provide structural information on the characteristic length scales of the superlattice, the modulation wavelength Λ and the lattice spacing. Because the scattered x-ray intensity is measured, the phase information is lost. It is impossible to directly convert the measured intensities to obtain the structure. Modeling of the superlattice is required to compare the calculated intensity of the modeled superlattice with the measured intensity. By fitting the measured intensity profiles with model calculations it is possible to obtain the structure. This type of structural characterization is commonly used in x-ray and neutron diffraction from bulk powder crystals using the Rietveld refinement procedure[2,3]. In

Mat. Res. Soc. Symp. Proc. Vol. 229. ©1991 Materials Research Society

Rietveld refinement, the structure of a single unit cell is modeled and the relative intensity of the diffraction peaks is determined from the structure factor of the unit cell. The difference with the present refinement technique is that here the relative intensities *and* the line profiles are used to determine the average unit cell *and* the statistical deviations from this average.

In many superlattices, the structural coherence length, ξ, derived from the full width at half maximum of diffraction peaks using Scherrer's equation, is limited to only a few times Λ, due to structural disorder. The type and amount of structural disorder can greatly affect the relative intensity of the diffraction peaks and disorder parameters need to be included in a model. Because many types of disorder can be present in a superlattice including layer thickness fluctuations, interface disorder, crystalline disorder, and interdiffusion, a large number of model parameters have to be included which makes a refinement procedure much more difficult.

In this paper we use a general kinematic diffraction model that includes both the average atomic structure of the layers and structural disorder to fit the measured x-ray diffraction profiles of a variety of superlattice structures. By fitting the measured profiles, it is possible to *quantitatively* determine both lattice constants and disorder parameters. We will present refinement results on a sputtered Mo/Ni superlattice in which disorder was introduced during growth and crystalline/amorphous Pb/Ge superlattices grown by molecular beam epitaxy. A detailed version of this work including a discussion of the theoretical approach, refinement procedure, and quantitative comparison of the refinement results of disorder, lattice parameters, and chemical composition with independent measurements has been submitted for publication[4].

THEORETICAL FORMALISM

To fit the measured x-ray diffraction profiles with a variety of structural models, we have developed a general kinematical expression, which includes both discrete and continuous cumulative disorder. Discrete disorder refers to fluctuations in layer thicknesses of which are an integer number lattice spacings. Continuous disorder refers to structural parameters that vary in a continuous way like the thickness of an amorphous layer.

The general model of a superlattice consists of a stack of M bi-layers of material A and B, as shown in Fig. 1. The layers are characterized by the structure factors F_{Aj}, F_{Bj} and thicknesses t_{Aj}, t_{Bj} of materials A, B in the j^{th} bi-layer and the interface distances separating the layers are given by a_{Aj} and a_{Bj}. The model in Fig. 1 explicitly includes only inter-layer disorder and no assumptions are made about the crystal structure of the layers. The one dimensional structure factor for a superlattice with M bi-layers with cumulative layer thickness fluctuations can be written as :

$$F(q) = \sum_{j=1}^{M} \exp(iqx_j)\left(F_{Aj} + \exp(iq(t_{Aj} + a_{Aj}))F_{Bj}\right)$$

$$\text{where } x_j = \sum_{s=1}^{j-1} t_{As} + a_{As} + t_{Bs} + a_{Bs} \qquad (1)$$

and q is the scattering vector given by $q = 4\pi\sin(\theta)/\lambda_x$. The scattering intensity is given by $I(q)=\langle F(q)F^*(q)\rangle$ [5] where the brackets are an ensemble average over all possible F_{Aj}, F_{Bj}, t_{Aj} ,t_{Bj}, a_{Aj}, and a_{Bj}. The expression for I(q) can be written in a closed form if each layer is assumed to be statistically independent in a similar fashion as the original intensity calculations by Hendricks and Teller[6] which included the effects of random sequencing of layers.

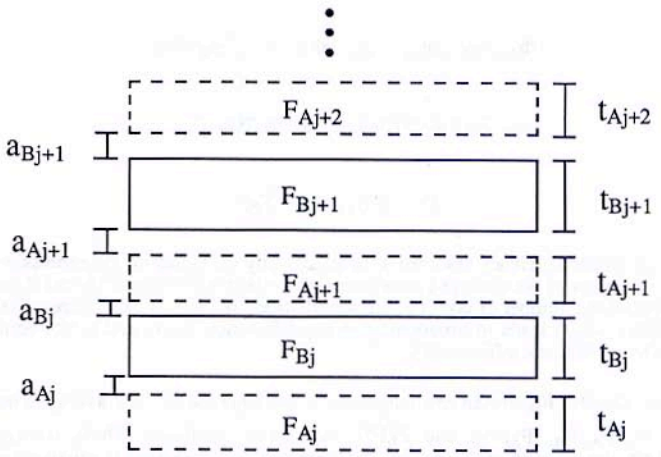

Fig. 1: Representation of a superlattice consisting of layers of materials A and B, with thicknesses $t_{A,j}$, $t_{B,j}$ and structure factors $F_{A,j}$, $F_{B,j}$. The layers are separated by interface distances $a_{A,j}$ and $a_{B,j}$.

For a lattice mismatched incoherent interface, the lattice positions are not well defined which leads to variations in the interface distance. Therefore, we will assume that the interface distances a_{Aj} and a_{Bj} vary in a continuous manner, as was done in our previous work.[7,8] To simulate such variations, a Gaussian distribution of width c about an average interface value a is assumed for both interfaces a_A and a_B. The intensity for a superlattice with M bi-layers can be written as:

$$I(q) = M\Big[\langle F_A F^*_A\rangle + 2\,\mathrm{Re}\left[e^{\zeta}\,\Phi_A\,\overline{F}_B\right] + \langle F_B F^*_B\rangle\Big]$$

$$+\ 2\ \mathrm{Re}\Big[\Big\{e^{-\zeta}\Phi_B\,\overline{F}_A T_A^{-1} T_B^{-1} + \Phi_A\,\overline{F}_A\,T_A^{-1} + \Phi_B\,\overline{F}_B\,T_B^{-1} + e^{\zeta}\Phi_A\,\overline{F}_B\Big\} \tag{2}$$

$$\times\ \left\{\frac{M - (M+1)\,e^{2\zeta}T_A T_B + \left(e^{2\zeta}T_A T_B\right)^{M+1}}{\left(1 - e^{2\zeta}T_A T_B\right)^2} - M\right\}\Big]$$

where $\zeta = iqa - q^2c^2/2$, Re designates the real part of the term in the bracket and the following averaged parameters are defined by:

$$\Phi_A = \langle \exp(iqt_A) F^*_A \rangle , \quad \Phi_B = \langle \exp(iqt_B) F^*_B \rangle$$

$$T_A = \langle \exp(iqt_A) \rangle , \quad T_B = \langle \exp(iqt_B) \rangle \tag{3}$$

$$\overline{F}_A = \langle F_A \rangle , \quad \overline{F}_B = \langle F_B \rangle$$

Because the layers are assumed to be statistically independent, the expression for I(q) can be written in terms of the averaged parameters of the layers of material A and B (equation (3)) independent of the number of layers in the superlattice. We would like to stress that all disorder is cumulative which leads to broadening of the diffraction peaks and is not equivalent to an effective Debye-Waller coefficient[5].

To calculate I(q) for an explicit model using equation (2), the averaged quantities Φ_A, Φ_B, T_A, T_B, $\overline{F}_A$, $\overline{F}_B$, $\langle F_A F^*_A \rangle$, and $\langle F_B F^*_B \rangle$ have to be calculated. These averaged quantities include both the average structure of the layers and the statistical fluctuations of the layers throughout the superlatice. For discrete disorder, the averages can be calculated by summing over all the possible F_{Aj} and F_{Bj} with corresponding t_{Aj} and t_{Bj} weighted by the probability of occurrence. Continuous disorder requires integration of the bracketed quantity over all the possible values of the continuous variable weighted by the probability of occurrence. The effect of these fluctuations on the x-ray diffraction profile of a superlattice is determined by the parameters of a single unit cell. The specific type of structural order within a layer can be crystalline, amorphous, or any other suitably chosen structure and equation (2) can be shown to agree with previous model calculations when a suitable crystal structure is chosen[5-11].

The model we use for a crystalline layer allows for variation of the lattice constant near the interface as shown in Fig. 2. The crystalline layer is described by N atomic planes which are separated by a lattice constant d. Three atomic planes near the interface are allowed to expand or contract an amount $\Delta d_1 e^{-n\alpha}$ and $\Delta d_2 e^{-n\alpha}$, where n=0,1,2 corresponds to the first, second, and third atomic plane away from the interface. α is the constant that determines the decay of the strain away from the interface and is typically assumed to be 0.5. The structure factor for this layer is given by:

$$F_j(q) = f\left[1 + \exp\left(iq\left(d+\Delta d_1\right)\right) + \cdots + \exp\left(iq\left((N_j-1)d+\left(\Delta d_1+\Delta d_2\right)\left(1+e^{-\alpha}+e^{-2\alpha}\right)\right)\right)\right] \tag{4}$$

Each layer is assumed to have an integer number of planes which varies about an average value $\overline{N}$. The average number of planes does not have to be restricted to an integer value. The distribution of the number of planes N_j for material A and B is given by a discrete distribution about the mean values $\overline{N}_A$ and $\overline{N}_B$ with widths s_A and s_B. For large values of s, the distribution approximates a Gaussian distribution, and for small values the weighted average of the nearest integers. The terms in equation (3) are determined by averaging the quantities within the brackets for various N_j weighted by the probability of occurrence.

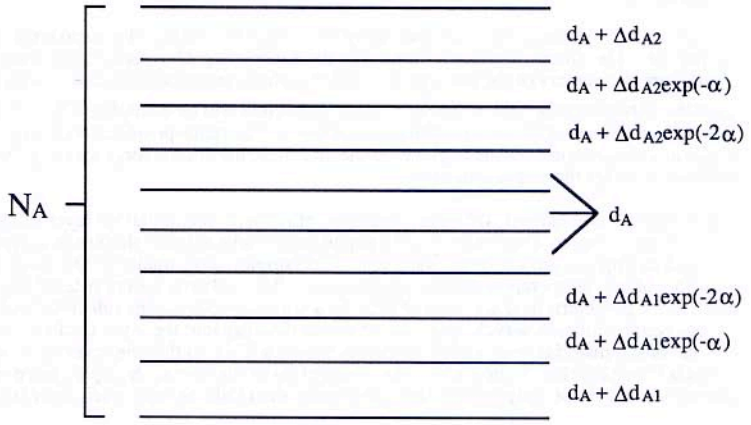

Fig. 2 Representation of a crystalline layer which is strained towards the interfaces. Lines represent atomic planes. Δd_1, Δd_2, and α determine lattice deviation near the interface.

An amorphous layer such as Ge can be simulated by setting the scattering power of a layer equal to zero. To simulate a more intermediate amount of intra-layer disorder between a perfectly crystalline and amorphous layer, the positions of the atomic planes of a crystalline layer are allowed to vary randomly. If the random variations of the planes are non cumulative, the effect of the variation will be equivalent to thermal fluctuations and can be modeled by an effective Debye-Waller parameter multiplied to the scattering factor of the layer. If the disorder is cumulative, the scattering factor of a layer with N atomic planes with lattice spacing d is given by:

$$F = f \sum_{j=0}^{N-1} \exp\left(iq\left(jd + \sum_{r=1}^{j} \partial_r\right)\right) \tag{5}$$

where ∂_j is the deviation of the $(j+1)^{th}$ atomic plane. If the values ∂_j are assumed to vary independently in a continuous Gaussian distribution about zero with a width δ, the averaged terms in equation (2) for an integer value of N can be written as:

$$\overline{F} = f\left[\frac{1 - e^{N\beta}}{1 - e^{\beta}}\right], \quad \Phi = f^*\left[\frac{1 - e^{N\beta}}{1 - e^{\beta}}\right], \quad T = e^{(N-1)\beta}$$

$$\langle F\,F^* \rangle = ff^*\left[-N + 2\,\mathrm{Re}\left[\frac{N - (N+1)e^{\beta} + e^{(N-1)\beta}}{(1 - e^{\beta})^2}\right]\right] \tag{6}$$

where $\beta = iqd - q^2\delta^2/2$.

FITTING RESULTS

The refined parameters are determined by least squares fitting the measured x-ray diffraction profile. The fitting procedure used was the Levenberg-Marquardt algorithm [12] where the structure parameters of the average unit cell including statistical fluctuations (equation (3)) are adjusted to minimize χ^2, the difference of the calculated and measured profiles squared. All calculated intensities include an absorption correction and Lorentz-polarization factor. The scattering power of each atomic plane is given by the atomic scattering factor, including Debye-Waller coefficients, times the in-plane density.

To determine the sensitivity of x-ray structural refinement to cumulative layer thickness fluctuations, we have grown a series of Mo/Ni superlattices where layer thickness variations were introduced during the growth of the samples. The samples were made by DC magnetron sputtering onto ambient temperature silicon substrates[9]. The substrates were rotated over the targets and held for predetermined amounts of time by a computer controlled substrate holder to achieve the desired modulation wavelength. To introduce disorder into the layer thicknesses, the deposition time of the materials was varied randomly for each layer so that the layer thicknesses approximated a Gaussian distribution about the average layer thickness. Samples were made with thickness variations of only one of the constituent materials or with variations in both layers.

Mo/Ni can be grown as high quality superlattices, with the Mo bcc[110] and the Ni fcc[111] planes oriented perpendicular to the growth direction. X-ray scans were performed about the first order (bcc[110]/fcc[111]) and second order (bcc[220]/fcc[222]) portion of the x-ray profile. Examples of the diffraction profiles are shown in Fig. 3 for $[Mo(20Å)/Ni(22Å)]_{130}$ superlattices, where the values in parentheses refers to the average layer thickness and the subscript gives the total number of bi-layers. Figure 3a shows the diffraction profiles of a sample without artificial roughness and Fig. 3b and 3c for samples with 2.7 Å artificial roughness added to Ni and Mo respectively. The circles are the measured x-ray intensity and the solid line the structural refinement. The arrows indicate the expected peak positions for Mo and Ni. The effect of the additional disorder can be seen in both the relative intensity and linewidth of the profiles. As was predicted from earlier calculations[8], increased disorder of the Mo (Ni) layers leads to broadening of the superlattice peaks associated with Ni (Mo). The second order superlattice peaks are much more sensitive to discrete disorder. 2.7Å of artificial disorder is enough to almost completely suppress the second order high angle superlattice peaks.

The parameters used in the refinement were the interface distance a and continuous fluctuation width c, the average number of atomic planes $\overline{N}_{Mo}$ and $\overline{N}_{Ni}$, the standard deviation in layer thickness resulting from discrete disorder s_{Mo} and s_{Ni}, the lattice parameters d_{Mo}, Δd_{Mo1}, Δd_{Mo2}, d_{Ni}, Δd_{Ni1}, and Δd_{Ni2}. The exponential α that defines the decay distance of the lattice deviation away from the interface was set at $\alpha = 0.5$.

The results of the structural refinement values of s_{Mo} and s_{Ni} can be directly compared to the amount of additional artificial disorder introduced during growth. The samples without additional disorder have typical discrete disorder values of 1.0 Å indicating the layers vary on average less than one monolayer. The value of the continuous disorder was 0.18 Å which is in agreement with the values determined by Locquet et al.[7] and is close to the difference in the lattice spacing of Mo and Ni of 0.2 Å. The amount of additional structural disorder, determined from the fits shown in Fig. 3 from the first (second) order peaks, is for Ni 2.0 (3.3) Å and for Mo 1.0 (2.6) Å, which is in good agreement with the values added during growth. There is a small discrepancy between the values determined from the first and second order portion of the profiles, with the second order values in better agreement with the growth value. A possible explanation for the difference is that the second order peaks are much more sensitive to discrete disorder and should give a more accurate measure of the disorder for a small amount of

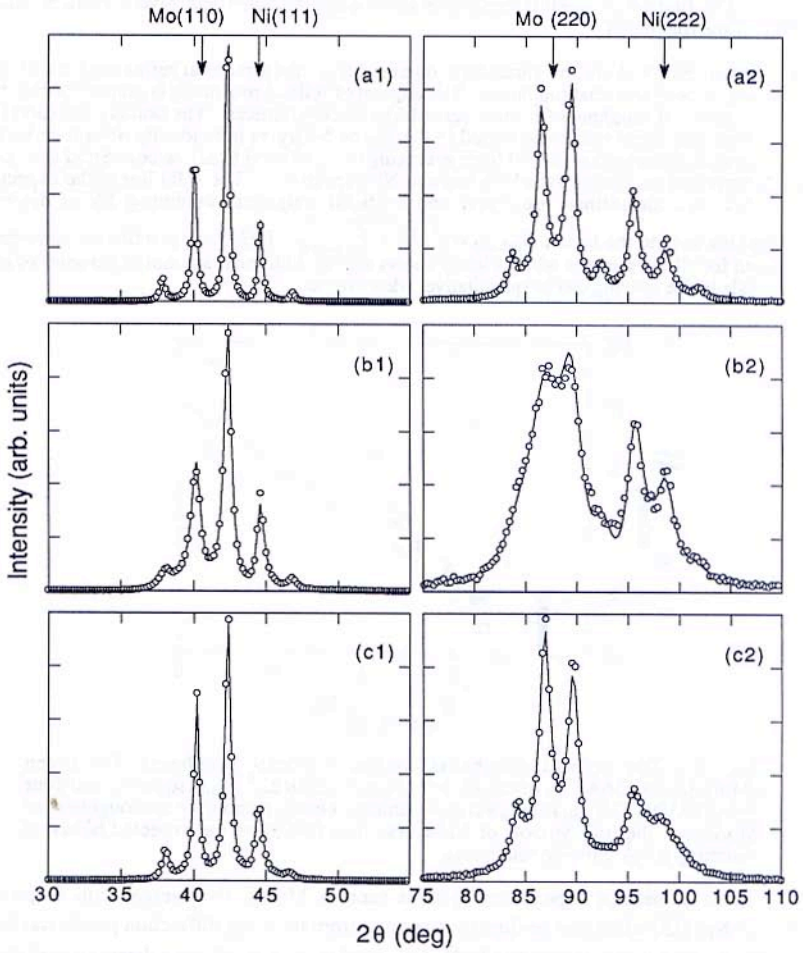

Fig. 3: Experimental profiles (o) and refined calculations (full lines) of three $[Mo(20Å)/Ni(22Å)]_{130}$ superlattices : (a) without artificial roughness, (b) with 2.7 Å artificial roughness on Ni and (c) 2.7 Å on Mo. The profiles on the left are taken around the first order main Bragg reflections, the profiles on the right around the second order.

additional disorder. When the amount of disorder increases, this is no longer true. In samples with an additional 3.3 Å of additional roughness, the second order superlattice peaks are no longer resolved. The refinement procedure can then only give a lower limit of the disorder (≈3.5Å). The first order satellite peaks are still clearly resolved and give a more accurate measure of the roughness.

Shown in Fig. 4 are the parameters obtained from the structural refinement for all the Mo/Ni samples with artificial roughness. The amount of refined roughness is graphed versus the amount of artificial roughness for three sets of Mo/Ni superlattices. The points correspond to samples with additional roughness added to the Mo or Ni layers individually or to both layers and represent an average determined from averaging the (111) and (222) values. Solid and open symbols represent roughness values on Mo and Ni respectively. The solid line is the expected relation between the refined roughness and artificial roughness assuming 1Å of discrete roughness intrinsic to the layers, $S_{refined} = \sqrt{1Å^2 + S^2_{artificial}}$. Excellent quantitative agreement is obtained for all the samples which clearly shows that an additional amount of disorder of less than a single lattice spacing can be quantitatively determined.

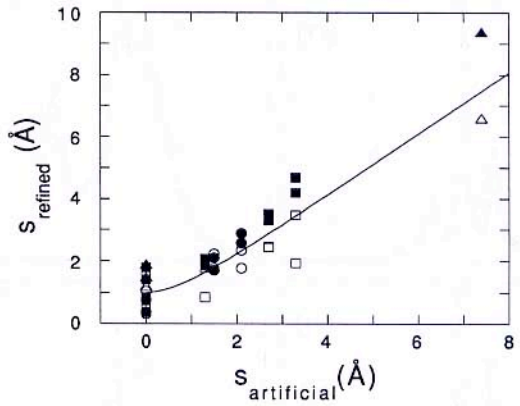

Fig. 4 The refined roughness versus artificial roughness for seven $[Mo(13Å)/Ni(16Å)]_{180}$ (circles), ten $[Mo(20Å)/Ni(22Å)]_{130}$ (squares) and four $[Mo(27Å)/Ni(33Å)]_{80}$ (triangles) superlattices. Open symbols are the roughness of Mo layers, the full symbols of Ni layers. The line gives the expected behavior assuming 1.0 Å intrinsic roughness.

In many metallic superlattice systems such as Mo/Ni, the average lattice spacing $\bar{d}=\Lambda/(N_A+N_B)$ [13] which can be directly measured from the x-ray diffraction profile has been found to expand with decreasing Λ [13,14]. Structural refinement allows a determination of the individual lattice spacing. Shown inFig. 5 is the refined values of the average Mo and Ni lattice spacing (the layer thickness divided by the number of layers) for the series of samples discussed in Fig. 3 and 4. There is systematic expansion in the Ni layer with decreasing Λ, with little change in the average Mo lattice spacing. This is consistent with the measured expansion in $\bar{d}$ [13].

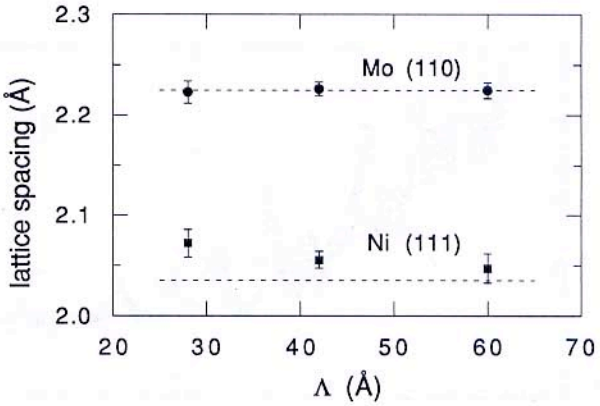

Fig. 5 Refined values for the average Mo (110) and Ni (111) lattice spacing for the same series of samples shown in Fig. 4. Error bars represent the standard deviation of the refined values all the samples at a given Λ. Dashed lines give the bulk values.

Some insight into the origin of the lattice expansion can be found by examining the refined values that determine the strain of the layer. Because of the interdependency of the individual lattice parameters of the layer d, Δd_1, and Δd_2, the uncertainty of these parameters tend to be larger than the uncertainty of the average lattice spacing shown in Fig. 5. However, clear trends in Δd_1 and Δd_2 above the uncertainty in the refinement can be obtained. For Mo, the strained parameters $\Delta d_{Mo1} = \Delta d_{Mo2} \approx -0.04 \pm 0.04$Å indicating very little strain in the Mo layers. In contrast, the Ni layers are asymmetrically strained with $\Delta d_{Ni1} \approx 0.13 \pm 0.05$Å and $\Delta d_{Ni2} \approx -0.04 \pm 0.04$Å. The asymmetry in the strain profile in the Ni is a common feature in the refinement of Mo/Ni superlattices. It is difficult to reproduce qualitatively some details of the x-ray profile without including the Ni strain profile. Δd_{Ni1} corresponds to the Ni-Mo interface where the Ni is grown on the Mo. This implies that much of the lattice expansion results from the growth of Ni on Mo in Mo/Ni superlattices.

The x-ray diffraction profile from MBE grown Pb/Ge superlattices were discussed extensively in a recent article by D. Neerinck et al.[11]. They found that by including both discrete and continuous random fluctuations in layer thickness, they could obtain good agreement with the high angle results in fitting the number of finite size maxima. But using the high angle results, no quantitative agreement could be reached for the low angle region, which shows more finite size structure than predicted by the fluctuations deduced from the high angle region. Shown in Fig 6a is the low angle spectrum for the [Pb (43Å)/Ge(38Å)]$_5$ superlattice. The calculated profile is calculated using a recursive optical theory [15-17] assuming 1Å of cumulative roughness on both layers. There is excellent agreement between the measured and calculated profile in both relative peak width and intensity. If the discrete disorder of the Pb layer is increased, both the finite size and Bragg peaks are broadened much more than the measured

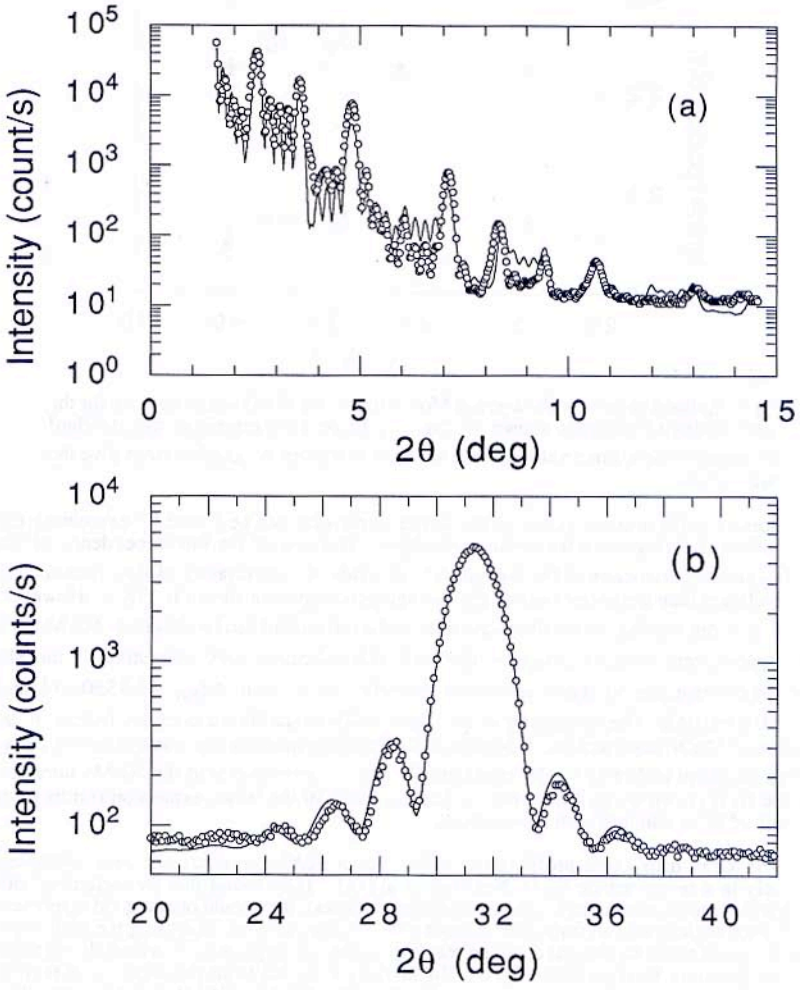

Fig. 6: (a) Low angle x-ray diffraction profile of a [Pb(45.4Å)/Ge(29.5Å)]$_5$ superlattice where the open circles are the measured intensity and the solid line is a simulation assuming 1Å of layer thickness fluctuation of both layers. (b) High angle profile of the same superlattice where open circles are the measured intensity and solid line is the refined profile.

profile. The limit of the discrete disorder as determined from the low angle profile is ≈2Å which is smaller than the value determined by Neerinck et. al. from the high angle profile.

To understand the high angle profile requires the inclusion of intra-layer disorder described by equations (5) and (6). There are no indications of superlattice structure and only the finite size of individual Pb layers is observed resulting from the continuous disorder of the Ge layer[5]. The best fit results for the Pb layer is given by line in Fig. 6b. The Pb lattice spacing was 2.846Å. The asymmetry in the finite size peak intensities are explained by a slight lattice expansion near the interface of $\Delta d_{Pb1} = \Delta d_{Pb2} = 0.03$Å. The intra-layer disorder was $\delta = 0.06$Å and the discrete disorder was one monolayer (≈3Å). Although the discrete disorder values is higher than determined by low angle, it is much better agreement than the value determined without the inclusion of intra-layer disorder

A number of other Pb/Ge profiles with Pb thicknesses ranging from 40 - 90 Å were fit in a similar fashion and found that they were consistently best fit by including an intra-layer disorder of 0.04 - 0.06Å. The origin of the intra-layer disorder may arise from the low substrate temperature during growth (77K), which is needed to grow continuous thin (<250 Å) Pb films. The low temperature may inhibit the atoms mobility and the formation of a well defined crystalline structure.

CONCLUSION

We have developed a general procedure for the structural refinement of superlattices from the x-ray diffraction profiles which can provide quantitative information about the lattice spacing and disorder of the superlattice. A general kinematic diffraction formula, which includes lattice strains and random discrete and continuous disorder is combined with a non-linear fitting algorithm to fit the entire x-ray profile. The procedure is applied to a crystalline/crystalline Mo/Ni superlattices where disorder was introduced during the growth procedure. The amount of disorder is quantitative determined by refinement of the x-ray diffraction profile. By including intra-layer disorder, the diffraction profiles of MBE grown Pb/Ge superlattices can be fit quantitatively. The Superlattice Refinement from X-rays (SUPREX) program is available by writing to the authors (IKS or YB) directly.

This work was supported by DOE grant #DE-FG03-87ER45332 at UCSD and the Belgian Inter University Institute for Nuclear Science, the Inter University Attraction Poles and Concerted Action Programs at KUL. International travel support was provided by the Belgian National Science Foundation and NATO.

REFERENCES

[1] For recent reviews, see various articles in for instance Physics, Fabrication and Applications of Multilayered Structures, edited by P. Dhez and C. Weisbuch (Plenum Press, New York, 1988); Metallic Superlattices, edited by T. Shinjo and T. Takada (Elsevier, Amsterdam, 1987); I.K. Schuller, J. Guimpel, and Y. Bruynseraede, MRS Bulletin, Volume XV(2), 29 (1990). Synthetic Modulated Structures, edited by L.L. Chang and B. C. Giessen (Academic Press, New York, 1985).

[2] H.M. Rietveld, J. Appl. Cryst. 2, 65 (1969).

[3] F. Izumi, in Advances in the Rietveld Method, edited by R.A. Young (Oxford Univ. Press, in press).

[4] E.E. Fullerton, I.K. Schuller, H Vanderstraeten, and Y. Bruynseraede, Phys. Rev. B (submitted for publication)

[5] W. Sevenhans, M. Gijs, Y. Bruynseraede, H. Homma, and I.K. Schuller, Phys. Rev. B 34, 5955 (1986).

[6] S. Hendricks and E. Teller, J. Chem. Phys. 10, 147 (1942).

[7] J.-P. Locquet, D. Neerinck, L. Stockman, Y. Bruynseraede, and I.K. Schuller, Phys. Rev. B 39, 3572 (1988).

[8] J.-P. Locquet, D. Neerinck, L. Stockman, Y. Bruynseraede, and I.K. Schuller, Phys. Rev. B 39, 13338 (1989).

[9] I.K. Schuller, Phys. Rev. Lett. 44, 1597 (1980).

[10] B.M. Clemens and J.G. Gay, Phys. Rev. B 35, 9337 (1987).

[11] D. Neerinck, H. Vanderstraeten, L. Stockman, J.-P. Locquet, Y. Bruynseraede, and I.K. Schuller, J. Phys.: Condens. Matter 2, 4111 (1990).

[12] P.R. Bevington, Data Reduction and Error Analysis for the Physical Sciences, (McGraw-Hill, New York, 1969).

[13] M.R. Khan, C.S.L. Chun, G.P. Felcher, M. Grimsditch, A. Kueny, C.M. Falco, and I.K. Schuller, Phys. Rev. B 27, 7186 (1983).

[14] I. K. Schuller and M. Grimsditch, J. Vac. Sci. Technol. B 4, 1444 (1986).

[15] J.H. Underwood and T.W. Barbee, Appl. Opt. 20, 3027 (1981).

[16] D. Neerinck, K. Temst, H. Vanderstraeten, C. Van Haesendonck, Y. Bruynseraede, A. Gilabert and I.K. Schuller, Mat. Res. Soc. Symp. Proc. 160, 599 (1990).

[17] H. Vanderstraeten, D. Neerinck, K. Temst, Y. Bruynseraede, E.E. Fullerton, and I.K. Schuller, J. Appl. Cryst. (accepted for publication).